FUNDAMENTAL STUDY OF HEAT PIPE DESIGN FOR HIGH HEAT FLUX SOURCE

Ryoji Oinuma, Frederick R. Best
Department of Nuclear Engineering, Texas A&M University

ABSTRACT

As the demand for high performance small electronic devices has increased, heat removal from these devices for space use is approaching critical limits. A loop heat pipe(LHP) with coherent micron-porous evaporative wick is suggested to enhance the heat removal performance for the limited mass of space thermal management system. The advantage of LHPs to have accurate micron-order diameter pores which will give large evaporative areas compared with conventional heat pipes per unit mass. Also this design make it easy to model the pressure drop and evaporation rate in the wick compared with the evaluation of the heat pipe performance with a stochastic wick. This gives confidence in operating limit calculation as well as the potential for the ultra high capillary pressure without corresponding pressure penalty such as entrainment of the liquid due to the fast vapor flow. The fabrication of this type heat pipe could be achieved by utilizing lithographic fabrication technology for silicon etching. The purpose of this paper is to show the potential of a heat pipe with a coherent micron-porous evaporative wick from the view point of the capillary limitation, the boiling limitation, etc. The heat pipe performance is predicted with evaporation models and the geometric design of heat pipe is optimized to achieve the maximum heat removal performance per unit mass.

INTRODUCTION

In recent years, the high thermal performance requirements for integrated circuits in computers, telecommunications, networking, and power-semiconductor markets are making high heat flux($> 100W / cm^2$) and improved thermal management critical needs.

Heat pipes are promising devices to remove thermal energy and keep the integrated circuits at the proper working temperature. The advantage of the heat pipe is in using phase change phenomena to remove thermal energy since the heat transfer coefficient of the phase change is normally 10-1000 times larger than typical heat transfer methods such as heat conduction, forced vapor or liquid convection. Even though a heat pipe has a big potential to remove the thermal energy from a high heat flux source, the heat removal performance of heat pipes cannot be predicted well since a first principles of evaporation has not been established.
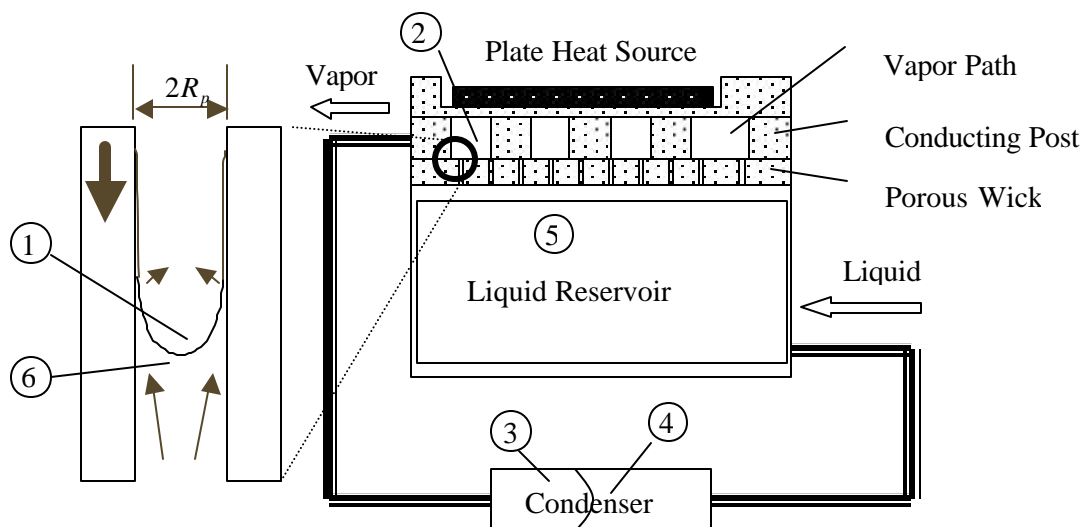
Figure 1: Loop Heat Pipe with coherent porous wick

Since the porous material used for current heat pipes is usually stochastic structure, it is hard to apply analytical or numerical methods for design optimization. A loop heat pipe with coherent pores integrated to the heat source is considered as a calculation model in this paper(Fig.1). The advantage of this design is to have accurate micron-order diameter pores which will give large areas of evaporative thin film more than in conventional heat pipes. Also this design make it easy to calculate pressure drop and evaporation rate in the wick compared with the evaluation of the heat pipe performance with the stochastic wick, which bring us to the confidence in operating limit and potentially the ultra high capillary pressures without corresponding pressure penalty such as entrainment of the liquid due to the fast vapor flow.

The thermal energy from the heat source conducts through the post to the body of evaporator and the heat is removed by evaporation of working fluid in pores driven by capillary forces. The post connecting the heat source and the evaporator is made of silicon and the evaporator consists of silicon around the evaporative region and silicon dioxide below it to prevent boiling in the liquid reservoir (Figure 2). The diameter of evaporative pores is micron order and the pitch between pores is a few times larger than the pore diameter. The height of the post, thickness of evaporator body is order of hundreds microns. The fabrication of this type heat pipe could be achieved by utilizing micro electro mechanical systems (MEMS) fabrication technology which is silicon etching. Also the evaporator will have micro-machine multiple layers to prevent boiling at the bottom of the wick.
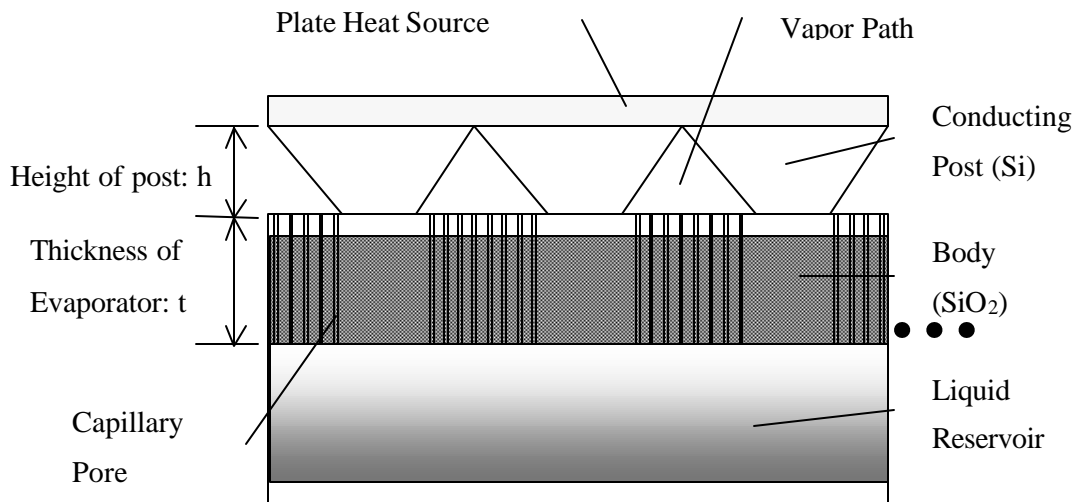
Figure 2: Coherent Porous Evaporator (Side View)

DEFINITION OF GEOMETRIC PARAMETERS

Figure 3 shows the top view of the coherent porous evaporator. The evaporator consists of a number of unit cells which has a unit length of w, pitch of P and number of pores of n, pore diameter of d. The width of conducting post connecting between the heat source and the evaporator is b. These parameters have relations:

$$w = b + nP$$

$$h = \frac{\sqrt{3}}{2}nP \qquad (1)$$
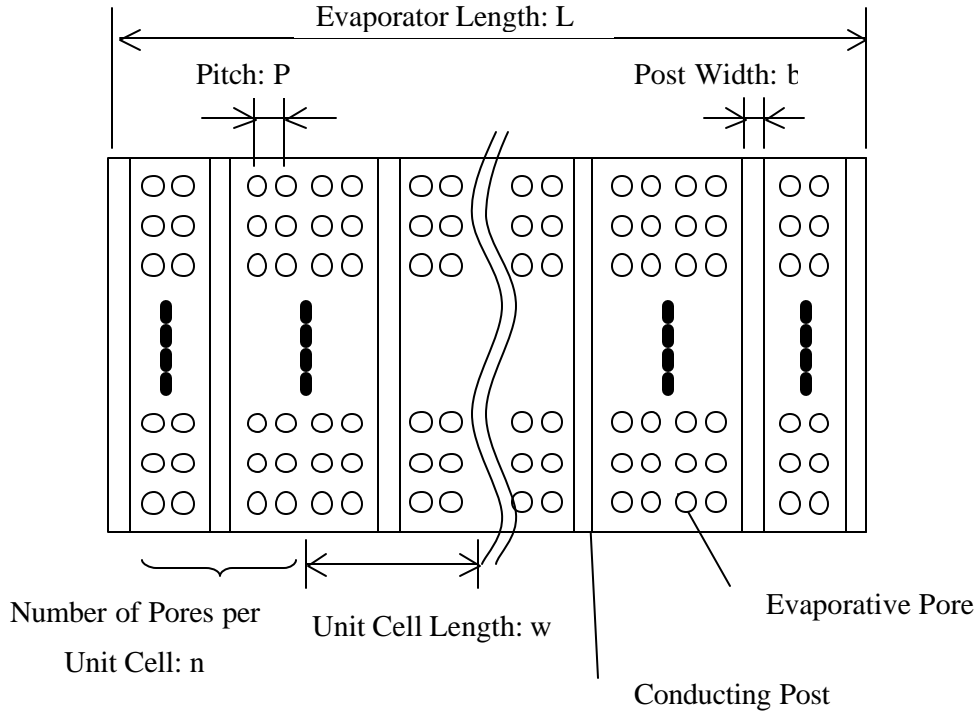
Figure 3: Top view of Coherent Porous Evaporator

To simplify the problem, the following parameters are defined

$$C_p \equiv P/d$$

$$C_b \equiv b/w \qquad (2)$$

and parameters will be given again as

$$b = \frac{nC_p d}{(1/C_b - 1)}$$

$$h = \frac{\sqrt{3}}{2}nP = \frac{\sqrt{3}}{2}nC_p \qquad (3)$$

In the calculation, n and d are fixed and C_b, C_p will be varied to change the geometry.

METHOD

OVERVIEW OF CALCULATION
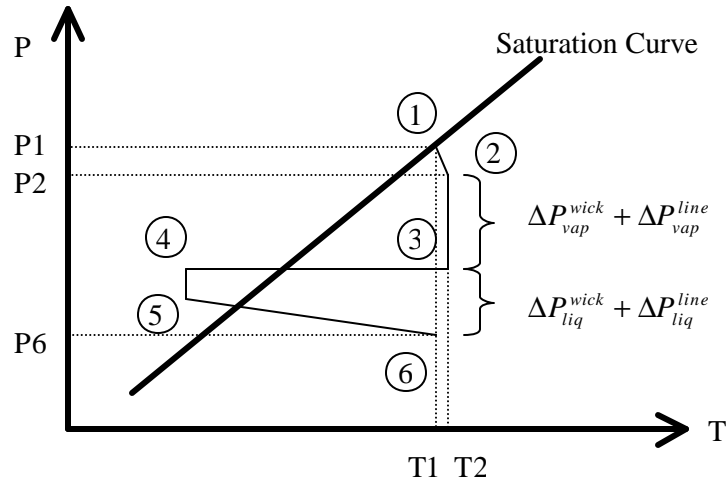
Figure 4 : Operating Cycle of Loop Heat Pipe

Figure 4 shows the operating cycle of a Loop Heat Pipe[1]. The heavy line is the saturation curve for the working fluid. Point 1 corresponds to the vapor condition just above the evaporating meniscus surface and Point 2 corresponds to the bulk vapor condition in the vapor path. Point 3 corresponds to the vapor pressure at the exit of the vapor path and the Point 4 corresponds to the vapor in the condenser. Point 5 corresponds to the liquid state in the condenser and Point 6 corresponds to the superheated liquid just below the meniscus interface. The heat pipe will satisfy the following conditions to operate.

$$P2 - P6 = \Delta P_{liq}^{wick} + \Delta P_{vap}^{wick} + \Delta P_{liq}^{line} + \Delta P_{vap}^{line} \tag{4}$$

$\Delta P_{liq}^{wick}, \Delta P_{vap}^{wick}$ are the liquid pressure and vapor pressure drops in the evaporator. $\Delta P_{liq}^{line}, \Delta P_{vap}^{line}$ are the liquid and vapor pressure drops in the transport line. All of pressure drops are supposed to be a function of a heat flux generated by the heat source and geometric parameters such as w, b, n, P in Figure 3. Since the evaporation rate in a pore can be determined by pressure and temperature of liquid and vapor near the

interface, the evaporation rate in a pore is a function of these values. If we define the effective evaporation rate per unit pore area, q'_{evap}, we will have a relation of

$$q'_{source} A_{source} = q''_{evap}(P2, T2, P6, T6) N(w, b, n, P) A_{pore}(d) \quad . \qquad (5)$$

q''_{source} is heat flux generated by the heat source. A_{source} and A_{pore} are the area of the heat source and a pore. N is the total number of pore in an evaporator and will be given as

$$N = \frac{L^2}{wP} n \qquad (6)$$

Since the area of a pore is a function of the diameter of pore and the number of the pore is a function of geometry parameter of evaporator (Figure 3), N varies due to the geometry of the evaporator. It will be assumed that the temperature increase(T2-T1) of the steam in the vapor path due to the heat transfer from the conducting wall or the heat source is small so that $T1 = T6 \approx T2$. We set T2=T6=constant. P6 is assumed to be equal to the saturation pressure at the temperature of condenser(T5). This is based on the fact that Point 5 could not be far from the saturation curve and the pressure drop from Point 5 to 6 is not large compared with the saturation pressure at T5. P2 will be obtained for a provided geometry to satisfy equations (4) and (5). This chapter shows the way to calculate the effective evaporation rate per unit pore area(q'_{evap}) and the pressure drops(P2-P6) to solve equations (4) and (5).

PHENOMENA IN A PORE

According to Potash and Wayner (1972)[2], in a micron scale pore, a meniscus is formed The meniscus is divided into three regions: non-evaporating region, thin film region and intrinsic region (Figure 4). In the non-evaporating region, the intermolecular dispersion force (Van der Waals force) between liquid molecules and wall molecules are strong enough to prevent evaporation from the liquid-vapor interface. The intermolecular force is also known as the disjoining pressure. In the thin film region, the intermolecular force holds the liquid molecules, but not as strong as to prevent evaporation, so evaporation is occurring. If we assume the heat conduction between the wall and the liquid interface is one dimensional, the interfacial temperature is dependent on the distance between the wall and the interface and liquid properties. The interfacial temperature gives the evaporation rate. The liquid thickness of this region is about the order of nano-meter. In

the intrinsic meniscus region, the surface tension is dominant and the meniscus is formed. The evaporation rate per unit area is relatively smaller than in the thin film region.
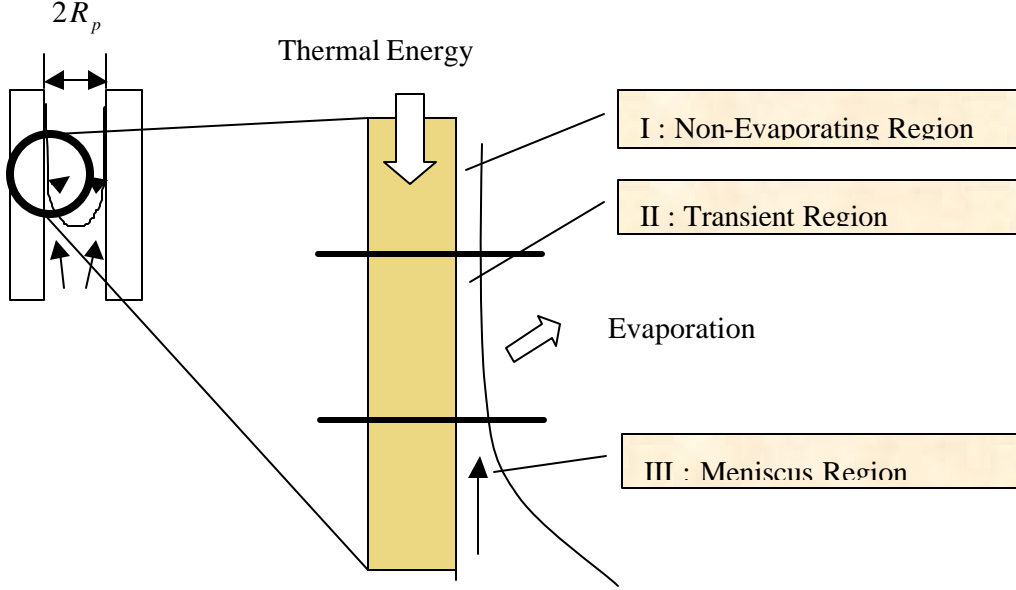
Figure 4: Classification of Evaporating Region

GOVERNING EQUATION

The meniscus profile and the evaporation rate along the meniscus interface can be calculated by solving Navier-Stokes equation (DasGupta, 1993)[3]. The momentum equation in Cartesian coordinate in the transition region is given by lubrication theory as

$$\boldsymbol{m}\frac{\partial^2 u}{\partial y^2} = \frac{\partial P_l}{\partial z} \qquad (7)$$

The boundary conditions are $u(R_{pore}) = 0$ at the wall and $\partial u/\partial y = 0$ at the interface. Integrating the momentum equation from $y = R_{pore} - \boldsymbol{d}(x)$ to $y = R_{pore}$ yields

$$u(y) = \frac{1}{2\boldsymbol{m}}\left(\frac{\partial p_l}{\partial z}\right)\left\{y^2 + 2(-R_{pore} + \boldsymbol{d}(z))y - R_{pore}(-R_{pore} + 2\boldsymbol{d}(z))\right\}. \qquad (8)$$

The mass flow rate at z=z will be

$$\Gamma = \boldsymbol{r}\int_{y=Rpore-\boldsymbol{d}(z)}^{y=Rpore} u(y)dy. \qquad (9)$$

From the mass balance, the evaporation rate from the interface matches the differential of the flow rate

$$\frac{d\Gamma}{dz} = -\dot{m} .$$
(10)

A evaporation model based on statistical rate theory has been suggested recently by Ward(1999)[4]. Since this model doesn't contain a evaporation or condensation coefficient as in the kinetic theory, we can avoid using an empirical value to evaluate the evaporation rate. The mass flux based on the statistical rate theory is given as

$$\dot{m} = \frac{M}{N_A} \frac{P_\infty(T_{li})}{\sqrt{2mkT_{li}}} \left\{ \exp\frac{\Delta S}{k} - \exp\frac{-\Delta S}{k} \right\}$$
(11)

, where

$$\frac{\Delta S}{k} = \frac{1}{k}\exp\left[\left(\frac{\boldsymbol{m}_l}{T_{li}} - \frac{\boldsymbol{m}_v}{T_{vi}}\right) + h_v\left(\frac{1}{T_{vi}} - \frac{1}{T_{li}}\right)\right]$$

$$= 4\left(1 - \frac{T_{vi}}{T_{li}}\right) + \left(\frac{1}{T_{vi}} - \frac{1}{T_{li}}\right)\sum_{l=1}^{3}\left(\frac{\Theta_l}{2} + \frac{\Theta_l}{\exp(\Theta_l/T_{vi})-1}\right) + \frac{\boldsymbol{n}_{l\infty}}{kT_{li}}\left(P_v - \frac{2\boldsymbol{s}}{Rc} - P_{sat}(T_{li}) - \frac{A}{\boldsymbol{d}^3}\right).$$

$$+ \ln\left[\left(\frac{T_{vi}}{T_{li}}\right)^4 \frac{P_{sat}(T_{li})}{P_v}\right] + \ln\left(\frac{q_{vib}(T_{vi})}{q_{vib}(T_{li})}\right)$$

$$q_{vib}(T) = \prod_{l=1}^{3}\frac{\exp(-\Theta_l/2T)}{1 - \exp(-\Theta_l/T)} .$$
(12)

k ($moleculeK/J$) is Boltzmann constant. $\boldsymbol{m}_l$, $\boldsymbol{m}_v$ (J/molecule) are the liquid and vapor chemical potential. T_{li}, T_{vi} are the interfacial liquid and vapor temperature. h_v (J/molecule) is the vapor enthalpy. $q_{vib}(T)$ is the vibrational partion function and Θ_l is the vibrational characteristic temperature which are 2290, 5160 and 5360(K)[5] for water. $v_{l\infty}$ ($m^3/molecule$) is the specific volume of the saturated liquid($m^3/molecule$).

The pressure balance between the liquid and the vapor at the interface is related by the augmented Young-Laplace equation as

$$P_v - P_l = \boldsymbol{s}K - \Pi$$
(13)

Π is the disjoining pressure given as

$$\Pi = \frac{\overline{A}}{\boldsymbol{d}^3}, \overline{A} = \frac{A}{6\boldsymbol{p}}$$

The curvature for the interface is give as

$$K = \frac{1}{2}\left[\frac{1}{(R_c - \boldsymbol{d})\left[1 + \left(\frac{d\boldsymbol{d}}{dz}\right)^2\right]^{1/2}} + \frac{\dfrac{d^2\boldsymbol{d}}{dy^2}}{\left[1 + \left(\frac{d\boldsymbol{d}}{dz}\right)^2\right]^{3/2}}\right]. \qquad (14)$$

Combining equations (7) through (14), we have

$$\boldsymbol{d}''' = -\frac{3}{rs\boldsymbol{d}^5}\left\{rs\boldsymbol{d}^4\boldsymbol{d}'\boldsymbol{d}''' - r\overline{A}\,\boldsymbol{d}\boldsymbol{d}'' + \dot{m}(\boldsymbol{d})m\boldsymbol{d}^2\right\}. \qquad (15)$$

If the heat conduction between the wall and the interface through the thin film is one dimensional, the interface temperature is

$$T_{li} = T_w - \frac{\dot{m}h_{fg}\boldsymbol{d}}{k_l}. \qquad (16)$$

The procedure to obtain the thickness of the film and the evaporation rate is as follows:

1. Determine the non-evaporating film thickness for $\dot{m} = 0$.

2. Determine the film thickness at the next vertical location ($z^{k+1} = z^k + \Delta z$) by solving equation (15) with fourth-order Runge-Kutta method.

3. By using the determined film thickness, obtain the evaporation.

4. Repeat 2 and 3 until the thin film region ends.

5. Determine the meniscus profile by the hemi-spherical shape

In the non-evaporation area, the temperature at the interface is equal to the wall temperature ($T_{li} = T_w$). The total evaporation rate per a pore is

$$Q_{total} = \sum_k\left\{\frac{\dot{m}(z^k) + \dot{m}(z^{k-1})}{2}h_{fg}(T_{li})\frac{R_c\Delta z}{\cos\left(a\tan\left(\dfrac{\boldsymbol{d}^{k+1} - \boldsymbol{d}^k}{\Delta z}\right)\right)}\right\}. \qquad (17)$$

If the total number of pores in evaporator is equal to N, the evaporation rate per unit evaporation area is

$$q''_{evap} = \sum_{n=1}^{N} Q_{total,N} \Big/ NA_{pore}. \qquad (18)$$

PRESSURE DROPS

Liquid Pressure Drop in the evaporator

The liquid is sucked due to the capillary pressure of pore from the bottom liquid reservoir to the top of the pore. To compensate the loss by the evaporation, the mass flow rate of the liquid in the pore should be balanced to the evaporation rate. The liquid pressure drop of the capillary tube in the evaporator for laminar flow is

$$\Delta P_{liquid} = f \frac{t}{d} \mathbf{r}_l \frac{V_p^2}{2} \tag{19}$$

$$Re = \mathbf{r}_l V_p \frac{d}{\mathbf{m}} \quad . \tag{20}$$

The mass flow rate in a unit cell of the evaporator is given as

$$q'_{source} Lw = h_{fg} \dot{m}_{cell}. \tag{21}$$

Since the number of pores in a unit cell is

$$n = \frac{L(w-b)}{P^2} . \tag{22}$$

Form the relationship between the mass flow rate per unit cell and one per pore, the mass flow in the pore is shown as

$$\dot{m}_{cell} = n \dot{m}_{pore} \tag{23}$$

$$\therefore \dot{m}_{pore} = \left(\frac{Lw - bL}{P^2} \right)^{-1} \frac{q''_{source} LW}{h_{fg}} = \frac{P^2}{(w-b)} \frac{q'_{source} Lw}{h_{fg}}.$$

The velocity in a pore becomes

$$V_p = \frac{4\dot{m}_p}{\mathbf{r}_l \mathbf{p} d^2} = \frac{4P^2}{\mathbf{r}_l \mathbf{p} d^2 (w-b)} \frac{q''_{source} w}{h_{fg}}. \tag{24}$$

Reynolds's number is also deformed to

$$Re = \frac{\mathbf{r}_l d}{\mathbf{m}} \frac{4P^2}{\mathbf{r}_l \mathbf{p} d^2 (w-b)} \frac{q''_{source} w}{h_{fg}} = \frac{4P^2 q''_{source} w}{\mathbf{m}_l \mathbf{p} d(w-b) h_{fg}}. \tag{25}$$

For laminar flow, the friction factor is

$$f = \frac{64}{\text{Re}} . \tag{26}$$

Substituting from equation (24) to (19), the liquid pressure drop is

$$\Delta P_{liquid} = \frac{64}{\text{Re}} \frac{t}{d} \boldsymbol{r}_l \frac{V_p^2}{2} = \cdots = \frac{32 \boldsymbol{m}_l}{\boldsymbol{r}_l h_{fg} \boldsymbol{p}} \frac{P^2 wt}{d^4 (w-b)} q''_{source} . \tag{27}$$

Vapor pressure drop in the evaporator

As shown in Figure 2, the cross sectional shape of the vapor path in the evaporator part is triangle, which is constrained due to the current lithographic technology. The flow rate is given as

$$\dot{m}_v = \boldsymbol{r}_v V_v A = \boldsymbol{r}_v V_v \frac{w-b}{2} h . \tag{28}$$

Therefore, the vapor velocity is

$$V_v = \frac{\dot{m}_v}{\boldsymbol{r}_v A} = \frac{\dot{m}_v}{\boldsymbol{r}_v} \frac{2}{(w-b)h} = \frac{2}{\boldsymbol{r}_v (w-b)h} \frac{q''_{source} Lw}{h_{fg}} . \tag{29}$$

It will be checked whether the vapor velocity will exceed the speed of sound or not when the maximum heat removal ability is determined. If it exceed, the vapor velocity is set to the sound of speed and the maximum heat removal ability of the evaporator is calculated with it.

The friction factor for the equilateral triangle (White, 1991)[5] is

$$C_f = \frac{13.333}{\text{Re}_{Dh}} = \frac{13.333}{r V_v D_h / \boldsymbol{m}_v} = \frac{13.333 \boldsymbol{m}_v}{\boldsymbol{r}_v D_h} \frac{\boldsymbol{r}_v (w-b)h}{2} \frac{h_{fg}}{q'_{source} Lw} \tag{30}$$

, where

$$D_h = \frac{a}{\sqrt{3}} = \frac{2}{3} h \tag{31}$$

Actually, the some vapor is generated at the middle of evaporator and others are generated near the exit of the vapor path and the pressure drop is dependent on the location where the vapor is generated. Since we want to know the performance limitation due to the pressure drop and the sonic limitation, the maximum pressure drop should be considered to evaluate the heat pipe performance. The vapor generated in the middle of the evaporator should be experienced the maximum pressure drop and we will

calculate it. The path length for this vapor is $L/2$ until the exit and the hydraulic diameter for the equilateral triangle is given as $D_h = a/\sqrt{3} = 2h/3$

By using above equations, the vapor pressure drop is given as

$$\Delta P_{vapor} = 4C_f \frac{L/2}{D_h} \mathbf{r}_v \frac{V_v^2}{2} = \ldots = \frac{51.96}{h^4} \frac{\mathbf{m}_v L^2 w}{\mathbf{r}_v h_{fg}} q'_{source}$$

$$\text{Re} = \frac{\mathbf{r}_v V_v D_h}{\mathbf{m}_v}$$

(31)

Vapor and Liquid Pressure Drop in Transport Line

The vapor and liquid pressure drop in the transport line are given as

$$\Delta P_{vap}^{line} = \frac{32 \mathbf{m}_v l}{D_v^4 \mathbf{r}_v \mathbf{p} h_{fg}} q''_{source},$$

(32)

$$\Delta P_{liq}^{line} = \frac{32 \mathbf{m}_l l}{D_{lv}^4 \mathbf{r}_l \mathbf{p} h_{fg}} q''_{source}.$$

(33)

LIMITATION OF HEAT PIPE PERFORMANCE

There are some limits to control the heat transfer of heat pipes (Faghri 1995)[1]: Capillary limitation, Sonic Limitation, Boiling Limitation, Viscous Limitation, Entrainment Limitation. These give information of the heat transfer limit due to the parameters such a pore diameter, a pitch between pores, number of pores between posts, thermophysical properties of working fluid (Figure 3).

For instance, the total pressure drop in the system is supposed to be lower than the capillary pressure to make the heat pipe work. The total pressure drop in the system is given by the sum of the pressure drop of liquid in pore, vapor in the exiting path over the evaporator, liquid and vapor transportation line to or from the condenser.

$$\Delta P_{cap} > \Delta P_{liq}^{wick} + \Delta P_{vap}^{wick} + \Delta P_{liq}^{line} + \Delta P_{vap}^{line},$$

(34)

If these pressure drops are expressed in geometric and thermophysical parameters of working fluid stated above, the equation (34) is expressed as

$$q'_{source} < \frac{2s}{r}\left[\frac{32\,\boldsymbol{m}_l P^2 wt}{\boldsymbol{r}_l h_{fg}\boldsymbol{p}d^4(w-b)} + \frac{51.96}{h^4}\frac{\boldsymbol{m}_v L^2 w}{\boldsymbol{r}_v h_{fg}} + \frac{32\,\boldsymbol{m}_v l}{D_v^4 \boldsymbol{r}_v \boldsymbol{p}h_{fg}} + \frac{32\,\boldsymbol{m}_l l}{D_l^4 \boldsymbol{r}_l \boldsymbol{p}h_{fg}}\right]^{-1},$$

where $w = nP + b$. (35)

$\boldsymbol{m}_l$ and $\boldsymbol{m}_v$ are the liquid and vapor viscosities, P is the pitch between pores, $\boldsymbol{r}_l$ and $\boldsymbol{r}_v$ are the liquid and vapor densities, d is the diameter of pore, D_l and D_v are the pipe diameter in the liquid and vapor transport lines, b and h are the width and height of the conducting post, l is the length of transport line, L is the horizontal length of evaporator, n is the number of pores between conducting posts. In the similar way for other limitations, the heat transfer limit will be calculated with these parameters.

TEMPERATURE DIFFERENCE BETWEEN HEAT SOUCE AND EVAPORATOR

Since the shape of vapor path is the right triangle, the height(h) can be determined if other parameters such as P, n, d, b are known. Therefore, the shape of the conducting post will be determined as well(Figure 2 and 3). The temperature difference between heat source and evaporator is given as

$$\Delta T_{wall} = 0.5q''_{source}(b + \frac{2h}{\sqrt{3}})\frac{\sqrt{3}}{k_{wall}L}\left\{\ln\left(\frac{3b + 2\sqrt{3}h}{3b}\right)\right\}. \qquad (36)$$

RESULT

GEOMETRY AND ASSUMPTIONS

We assume that we want to design the loop heat pipe which can remove the thermal energy from a heat source which generates a uniform heat flux and has the size of 1cm by 1cm, thus L=1cm. The evaporative pore diameter(d) is 10μm and the working fluid is water. The number of pores per unit cell(n) is set to 10. The thickness of the evaporator(t) is 200μm. Pitch between pores will be changed from $P = 1.1d$ to $P = 6d$ and the width of conducting post(b) varies between $b = 0.01w$ and

$b = 0.09w$. T2 is set to from 323.15 to 373.15K and P6 is assumed to be equal to the saturation pressure at $300K (\approx 4200 Pa)$. To simplify the problem, the temperature is uniform for the horizontal direction, the thermal contact resistances at the connection between the heat source and the conducting post or between the conducting post and the evaporator are ignored. The heat loss from the heat source by the radiation and convection is ignored also.

EVAPORATION AND MENISCUS PROFILE IN A PORE

The evaporation rate profiles along the axial position in a pore were calculated. Figure 5 shows the profile of the evaporation rate for the pore diameter of 10μm at T6=373.15K and $P_v = 9.0 \times 10^4$ Pa.
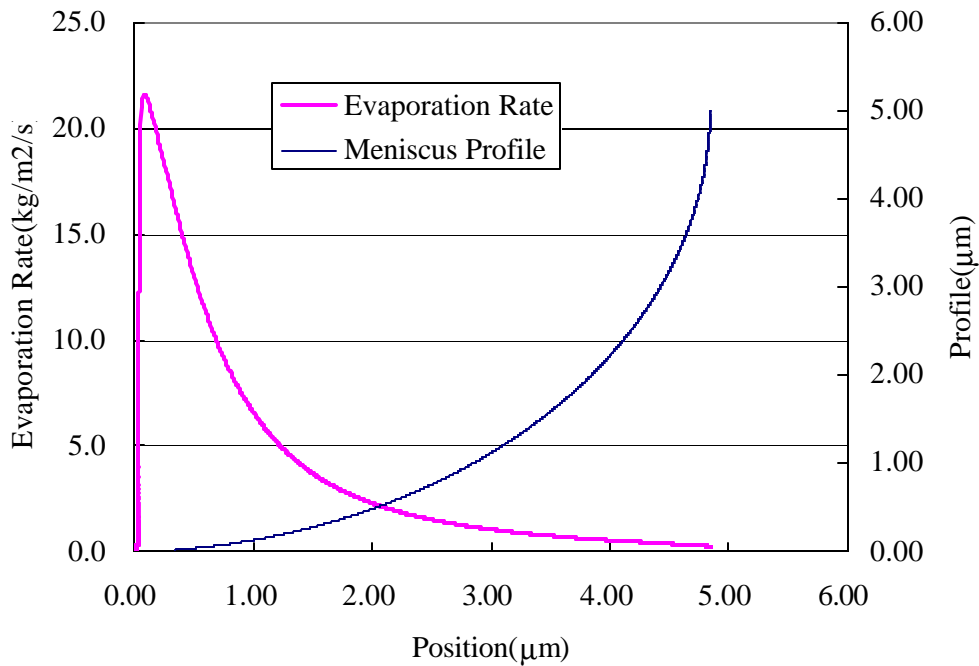
Figure 5: Profile of Evaporation Rate and Meniscus

(d=1.0e -5 m, T6=373.15K, Pv=9.0e4Pa)
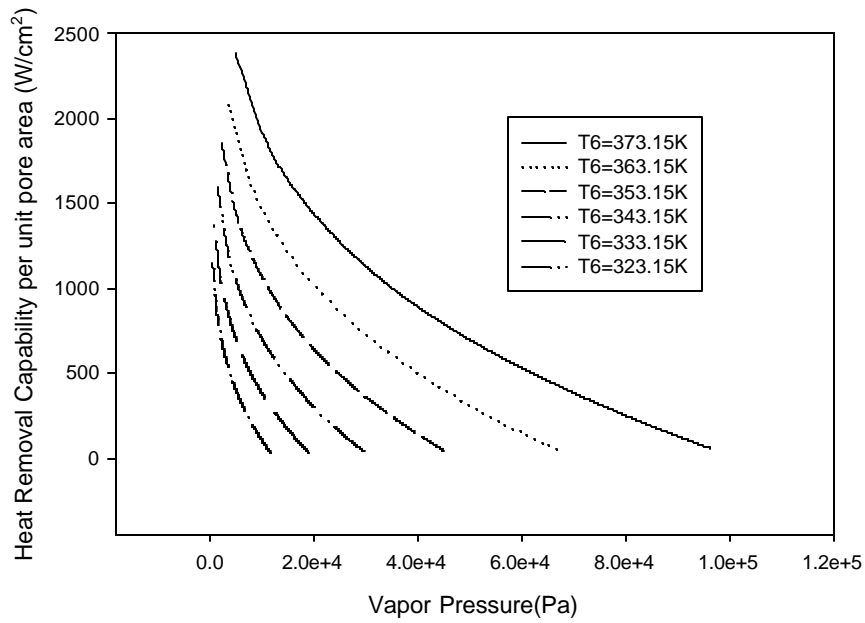
Figure 6: Heat Removal Capability per Pore Area(d=1.0e-5m)

Based on the calculation of evaporation rate in a pore, the heat removal capability in a pore is determined by using equations (17) and (18) and the results are shown on Figure 6 for several temperatures. Now we go back to equations (4), (5) and find q''_{source} to satisfy these equations. The results for several geometries are shown for T6=373.15 and T6=363.15K. Both figures show that the maximum heat flux is given at Cp(P/d)=2.1 and Cb(b/w)=0.01. In addition, we will find in both figures that q''_{source} increases as Cb decreases. This is reasonable as Cb is smaller, the vapor path is relatively larger, which cause to decrease the pressure drop. However, if the width of the conducting post are reduced too much, the temperature difference between the heat source and the evaporator will be large and the heat source temperature may exceed the limit.
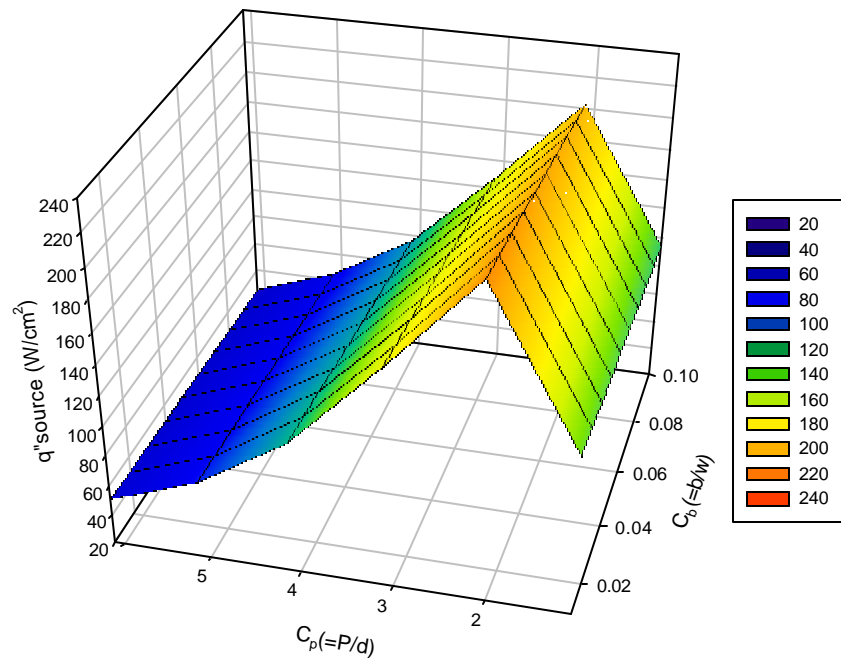
Figure 7: Heat Flux $(= q''_{source})$ to satisfy the operating condition for a given geometry

(T1=T6=373.15K and P6=Psat(T5=300K))

Usually thermal analysis requires designing a cooling system to keep the limit temperature of the heat source. For instance, the computer chips are required to sustain below the operating temperature and it is useless to design to exceed the limit temperature. Figure 9 shows the heat removal capability and the heat source temperature. If there is a heat source which has the limit temperature of 373K and generate the heat flux of 100W/cm^2, this heat pipe may satisfy these limitations.

Since our loop heat pipe system is operated only by the capillary force in the evaporator, the total pressure drop in the system cannot exceed the capillary pressure. The comparison between the total pressure drop and the capillary force are shown in Figure 10. The total pressure drops do not exceed the capillary pressure. The vapor pressure drop in evaporator is dominant and the liquid pressure drop is much lower than the

saturation pressure at T5 ($\approx 4200\,Pa$), which supports the assumption that the pressure at Point 5 is close to the pressure at Point 6.
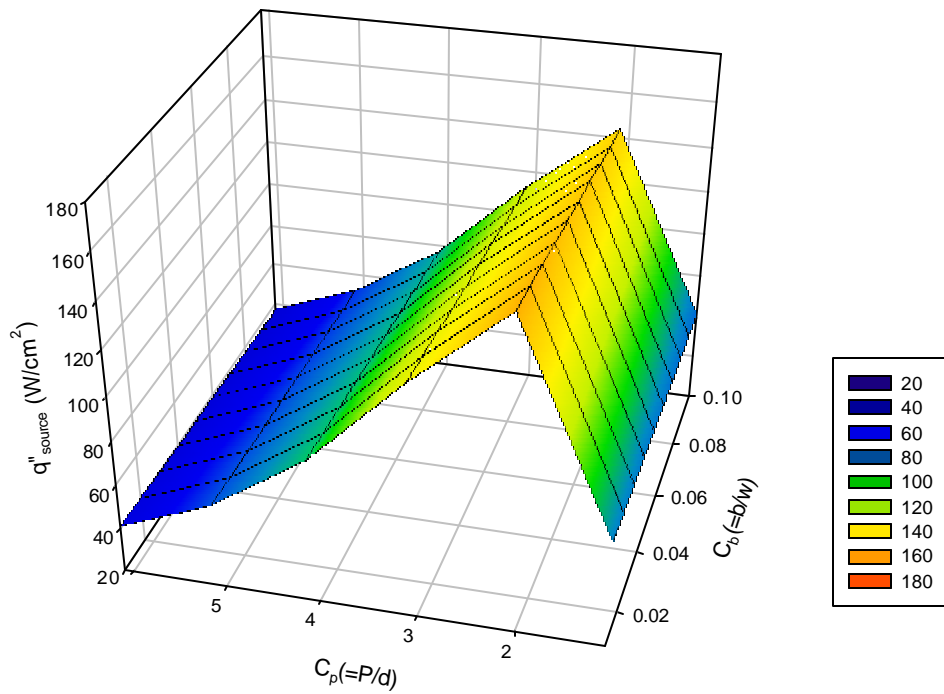
Figure 8: Heat Flux ($= q''_{source}$) to satisfy the operating condition for a given geometry

(T1=T6=363.15K and P6=Psat(T5=300K))
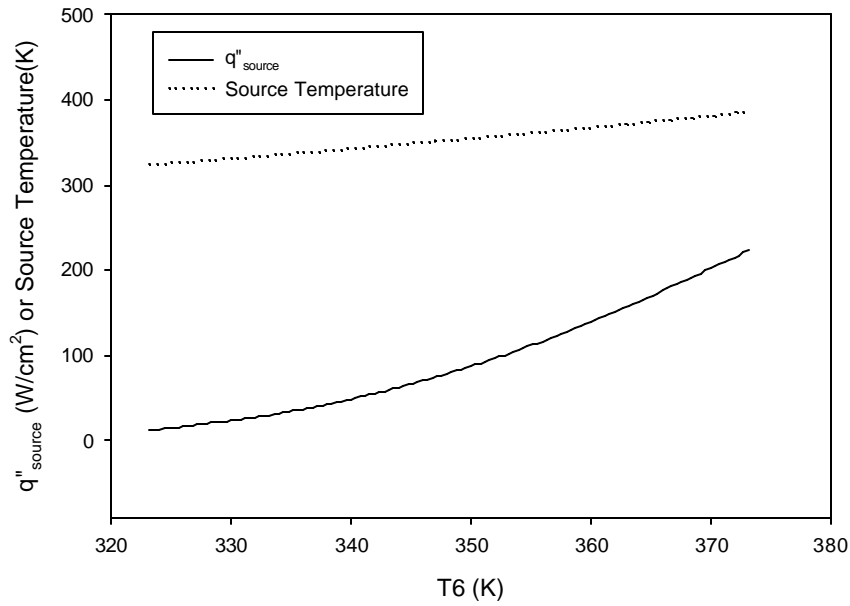
Figure 9: Heat Flux ($= q''_{source}$) and Heat Source Temperature for d=1.0e-5 m

(Cb=0.01, Cp=2.1, P6=Psat(T5=300K)
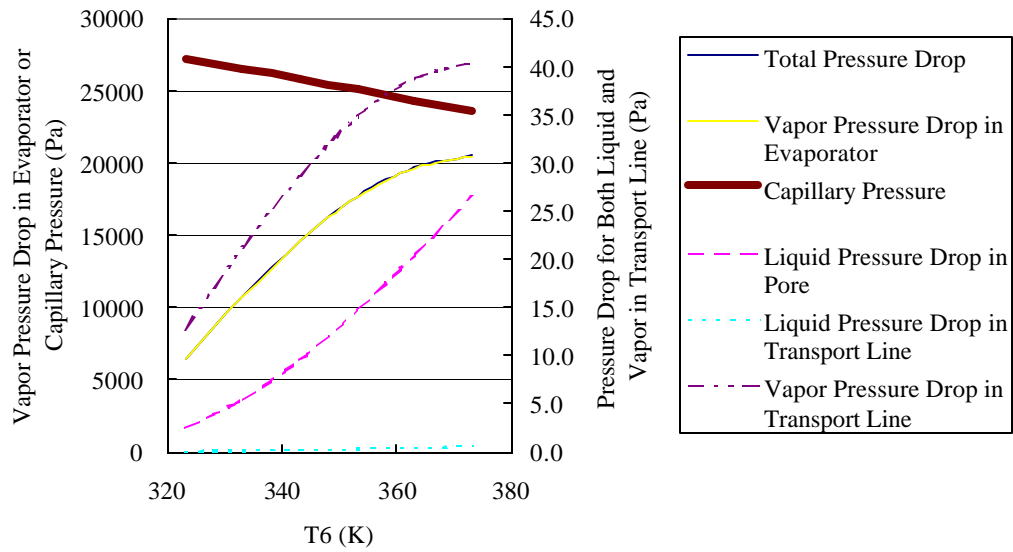
Figure 10: Total Pressure Drop and Capillary Pressure for d=1.0e-5 m

CONCLUSION

A loop heat pipe(LHP) with coherent micron-porous evaporative wick is suggested to enhance the heat removal performance and it is demonstrated that this design could achieve the high heat removal capability($>100W/cm^2$) with keeping the reasonable heat source temperature($<373.15K$) and satisfy the pressure limitation due to the pressure drop. The optimized geometric parameters can be found and the maximum heat flux is given at Cp(P/d)=2.1 and Cb(b/w)=0.01 for $d = 1.0 \times 10^{-5} m$ and n=10. In this paper, there are several assumptions which may not match the real condition. The most important things are that the temperature is uniform in evaporator. As far as our brief estimation with computational fluid dynamics calculation, the temperature across the evaporator varies and the evaporation rate of pores close to the conducting wall is higher than pores far from the conducting post. Also there are some unchanged geometric parameters such as pore diameter and number of pores in a unit cell because these parameters are strongly related to this problem and we avoid to discuss in this paper. In future, these things will be discussed in detail.

AKNOWLEDGEMENTS

NOMENCLATURE

A   Hamaker constant (J)

b   width of conducting post (m)

C_p P/d

C_b b/w

d   pore diameter (m)

D_l, D_v pipe diameter in transport line between evaporator and condenser

f   friction factor

h   height of conducting wall (m)

h_{fg}	latent heat (J/kg)
h_v	vapor enthalpy (J/kg)
k	Boltzmann constant (molecule K / J)
k_l	thermal conductivity for working liquid (W/mK)
k_{wall}	thermal conductivity (W/mK)
l	slit length (m)
M	molecular weight (kg)
n	number of pores per unit cell
N	total number of pores in an evaporator
N_A	Avogadro's number (1/mol)
P	pitch between pores or slits (m)
P_l	bulk liquid pressure (Pa)
P_{li}	liquid pressure at interface (Pa)
P_V	bulk vapor pressure (Pa)
P_{Vi}	vapor pressure at interface (Pa)
q'_{evap}	evaporation rate per unit horizontal pore area (W/ m^2)
q_{tatal}	total thermal energy from the heat source (W)
q'_{source}	thermal density of heat source (W/m^2)
Q	partial evaporation rate (W)
Q_{total}	total evaporation rate per pore or slit (W/pore)
R_{gas}	Universal gas constant (J/kg mol K)
R_{pore}	pore radius or half length of slit width (m)
S	enthoropy (J/kgT)
T_{li}	temperature at the interface of liquid side (K)
Tw	wall temperature (K)
T_V	vapor temperature (K)
T_{Vi}	vapor temperature at interface (K)
v_l	specific volume of liquid (m^3/kg)
V	velocity (m/s)
w	length per unit cell (m)
y	radial coordinate (m)
z	axial coordinate (m)

Γ	mass flow rate (kg/m)
δ	film Thickness (m)
ΔP	Pressure Drop (Pa)
ΔT	Temperature Difference (K)
Δz	distance between nodes for axial direction
μ_l	liquid chemical potential (J/kg/molecule) or liquid viscosity (Pa s)
μ_v	vapor chemical potential (J/kg/molecule) or vapor viscosity (Pa s)
ν	kinematic viscosity (m^2/s)
Π	disjoining pressure (Pa)
σ	surface tension (N/m)
θ	contact angle (Degree)

Superscriptions

k	index of z position
line	transport line between evaporator and condenser
wick	wick

Subscriptions

cell	unit cell
l or liq	liquid
li	liquid interface
p or pore	pore
sat	saturation condition
source	heat source
v or vap	vapor
vi	vapor interface
w or wall	wall
∞	saturation condition for flat interface

REFERENCES

1. Faghri, A, *Heat Pipe Science and Technology*, Washington, Taylor & Francis, (1995).

2. Potash, M., Jr. and Wayner, P. C., Jr., "Evaporation from a Two-Dimensional Extended Meniscus", *International Journal of Heatand Mass Transfer* **15**, 1851-1863 (1972).

3. DasGupta, S., Schonberg, J. A., Kim, I. Y. and Wayner, P. C., Jr., "Use of the Augmented Young-Laplace Equation to Model Equilibrium and Evaporating Extended Menisci", *Journal of Colloid and Interface Science* **157**, 332-342 (1993).

4. Ward, C. A., Fang G., "Expression for predicting liquid evaporation flux: Statistical rate theory approach", *Physical Review* E **59**, 429-440 (1999).

5. Carey, P. V., *Statistical Thermodynamics and Mircoscale Thermophysics*, Cambridge(U.K.), Cambridge University Press, (1999).

6. White, M. F., *Viscous Fluid Flow*, New York, McGraw-Hill, Inc, (1991).